JOURNAL OF APPLIED ELECTROCHEMISTRY 24 (1994) 798–802

Measurement of anode potentials at high current densities in $NaNO_3$ and $NaClO_3$ media by the current interruption method for metals used in aviation technology

J. HÍVEŠ,

Slovak Technical University, Department of Inorganic Technology, Radlinského 9, 812 37 Bratislava, Slovakia

I. ROUŠAR

Prague Institute of Chemical Technology, Department of Inorganic Technology, Technická 5, 166 28 Prague, Czech Republic

Received 28 September 1993; revised 23 January 1994

The *IR*-free anode potential of mild steel, nickel and four Ni–Cr–Fe alloys were studied at high current densities (1–100 A cm^{-2}) in $NaNO_3$ and $NaClO_3$ solutions. A constant current interruption technique was employed and the flow rate of the electrolytes was 14 m s^{-1} ($Re = 7370$). A plot of the anode potential against logarithm of current density yielded a Tafel line over a broad range of current densities. The plateau visible on the anode potential against current density curve was attributed to salt film formation. This explanation was confirmed by visual observation of the anode surface.

1. Introduction

Electrochemical machining (ECM) is a metal shaping process involving anodic dissolution of a metallic material at very high current densities and at high electrolyte velocities with small interelectrode gaps. Anodic polarization curves obtained for mild steel [1–4] and nickel [5, 6] in $NaNO_3$ and $NaClO_3$ solutions at high current densities show a linear dependency on the applied current densities, but the slope of the anodic polarization curves varies over a broad range, see Figs 1 and 2. For instance the IR-free anodic potential of mild steel varies from 1 to 7 V vs NHE at a current density of 100 A cm^{-2} in $NaNO_3$ solution and from 2 to 12 V vs NHE in $NaClO_3$ solution at the same current density. The main difficulty in measuring the anodic potentials at high current densities is to determine the voltage drop in the electrolyte (*IR* drop). The ohmic drop may represent several volts at high current densities and become a dominant term in the measured anode potential. A constant current interrupter technique is usually employed in the experimental determination of anode potentials during high-rate anodic dissolution of metals [1, 7–13].

The anodic dissolution of iron and nickel in $NaNO_3$ and $NaClO_3$ solutions has been studied by several authors [14–28]. Datta and Landolt [28] confirmed the important role of mass transport in high-rate transpassive dissolution of iron and nickel in concentrated ECM electrolytes. The anode potential, reaction stoichiometry and surface finish not only depend on the applied current density, but also on electrolyte flow conditions. The stoichiometry and current efficiency of iron dissolution in nitrate electrolytes is well known, current efficiency increases with increasing current density, but it is always less than 100% and increasing temperature decreases the dissolution efficiency of steel [4, 19, 20, 28, 29]. High-rate anodic dissolution of nickel in nitrate electrolytes under controlled hydrodynamic conditions has been investigated by Datta and Landolt [24–28]. They found that current efficiency for nickel dissolution is a function of current density and local nitrate concentration at the anode.

Chikamori *et al.* [1] found that the current efficiency for mild steel in $NaClO_3$ solutions exceeds 100% at higher current densities and the polarization curves exhibit negative slope, see Fig. 2. Mao and Chin [4] found that anodic dissolution of mild steel in $NaClO_3$ solutions takes place in three reaction stages depending on current density. From the shift of the polarization curves for 2 and 4 M $NaClO_3$ it follows that the rate of iron dissolution is proportional to the chlorate concentration.

The purpose of the present study was to evaluate the anodic potentials of mild steel, nickel, and Ni–Fe–Cr alloys in $NaNO_3$ and $NaClO_3$ solutions at high anodic current densities. The knowledge of the polarization curves is necessary for the calculation of the local current densities during ECM.

0021-891X

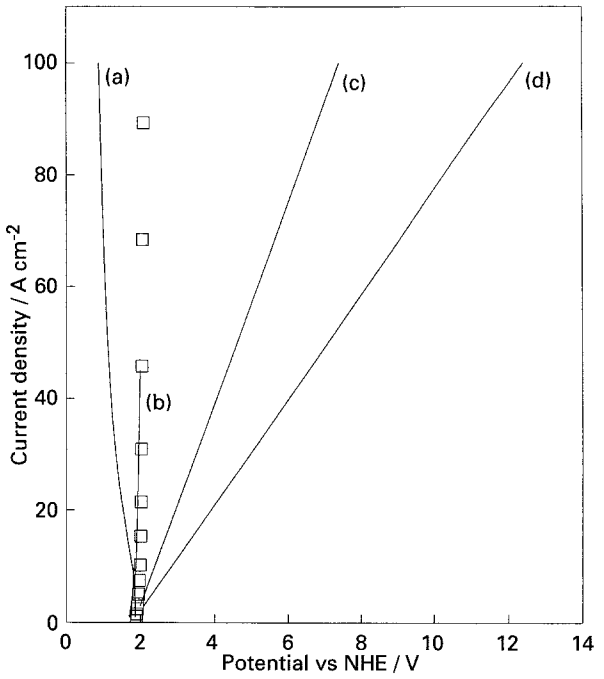

Fig. 1. Anodic polarization curves for mild steel electrodes in $NaNO_3$ solutions according to references (a) [1], (b) [2], (c) [3], (d) [3], (□) this work.

2. Experimental details

A flow-through cell was used; this is described in detail in [30]. A platinum wire of diameter 1.13 mm was used as a fixed cathode, which was positioned opposite the anode wire (composition see Table 1) of the same free electrode area (1 mm^2). For details of the cell see [30]. All measurements were performed galvanostatically after passing a charge of 20 C cm^{-2}. The current was then interrupted and transient anodic potential curves were recorded and stored every 50 ns by a fast transient recorder DL-912. Before the experiment, the anode surface was polished with a wet 600 grit grinding paper, rinsed with distilled water, and immediately transferred to the flow cell. A 20% $NaNO_3$ or 20% $NaClO_3$ solution was prepared from reagent grade $NaNO_3$ (LACHEMA, Brno) or pure $NaClO_3$ (CHZ, Sokolov) and distilled water. A fresh electrolyte was prepared for each anode material. All experiments were conducted at 25 ± 1 °C. The potential of the Ag/AgCl reference electrode was checked against a SCE before and after each run. Differences in the reference electrode potential during all experiments were less than ±2 mV.

3. Results and discussion

The measured voltage before interruption is a sum of the ohmic drop and the anodic potential. The evaluation of the anodic potential is based on the assumption that Tafel kinetics [30] are valid in these electrolytes. Details of the evaluation of the anodic potential (free of the *IR* drop), the ohmic drop, double layer capacity and the Tafel slope, are given in [30].

The confidence interval for the Tafel slope, *b*, is large owing to the contribution of the values calculated in the region near the critical current density, see [30]. Figs 3 and 4 show the *IR*-free anode potential against current density plot on a semilogarithmic scale for all metal materials used at a velocity of 14 m s^{-1} ($Re = 7370$). Apparently, *IR*-free anode potential is linearly related to the logarithm of the current density; this is in good

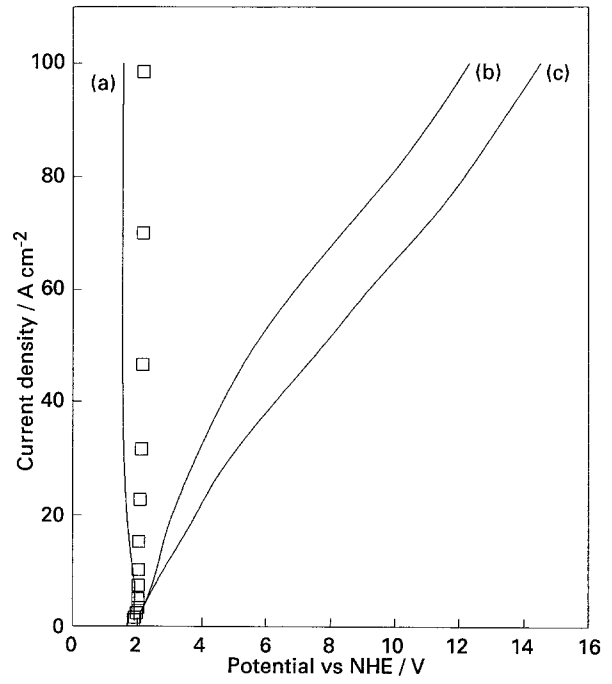

Fig. 2. Anodic polarization curves for mild steel electrodes in $NaClO_3$ solutions according to references (a) [1], (b) [4], (c) [4], (□) this work.

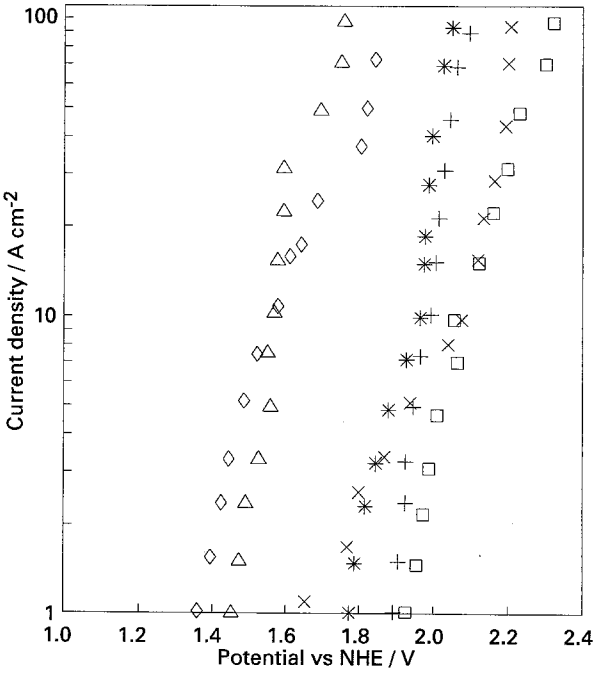

Fig. 3. Plot of *IR*-free anodic potential against current density in 20% $NaNO_3$. The linear flow velocity of the electrolyte was 14 m s^{-1}, $Re = 7370$. (+) Mild steel, (*) AK1, (□) nickel, (×) LVN10, (◇) EI437 and (△) EI617.

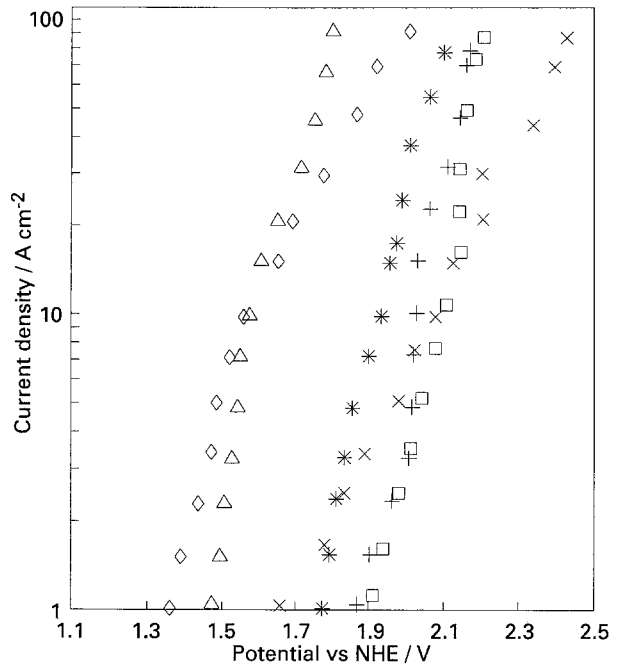

Fig. 4. Plot of *IR*-free anodic potential against current density in 20% $NaClO_3$. The linear flow velocity of the electrolyte was $14\,m\,s^{-1}$, $Re = 7370$. (+) mild steel, (*) AK1, (□) nickel, (×) LVN10, (◇) EI437 and (△) EI617.

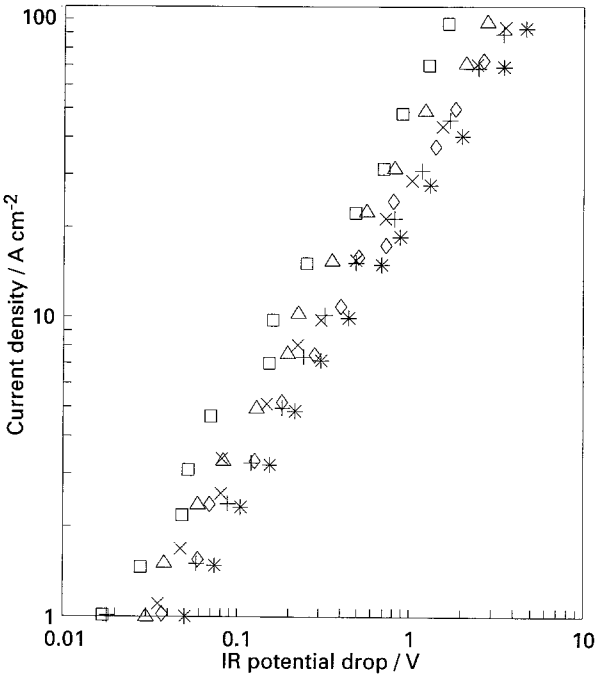

Fig. 5. Plot of *IR* potential drop against current density in 20% $NaNO_3$. The linear flow velocity of the electrolyte was $14\,m\,s^{-1}$, $Re = 7370$. (+) Mild steel, (*) AK1, (□) nickel, (×) LVN10, (◇) EI437 and (△) EI617.

agreement with the assumption about the Tafel behaviour of the investigated materials.

The critical current density is defined as the current density at which the concentration of salt on the anode surface reached the concentration of the saturated solution, followed by salt formation. When the critical current density is reached the polarization curve exhibit some distortion (plateau) due to salt film formation on the anode surface.

The polarization curve for mild steel in $NaNO_3$ exhibits linear behaviour without any distortion. Similar behaviour was observed with the material AK1, which is based on iron. The polarization curves measured for the materials based on nickel exhibit some distortion at the critical current density of approximately $40\,A\,cm^{-2}$, see Fig. 3 material EI437 and EI617. The shift of the *IR*-free anodic potential at higher current density represents about 150 mV. It may be assumed that this distortion corresponds to the limiting current density for the formation of a salt film on the anode surface. Visual observation of the anode surface after the experiments clearly showed that the surface of the anode obtained below the critical current density was porous and black. Above the critical current density, the surface of the

Table 1. Composition of the anode materials according to [32]

	AK1	*EI617*	*EI437*	*LVN10*	*Mild steel*	*Nickel*
Ni	1.65	74	74	74	—	99.9
Cr	11.25	14.5	20.5	12.5	—	—
Fe	82	5	1.0	0.5	98.64	0.1*
Al	—	2	0.8	6	—	—
Mo	0.42	3	—	4.5	—	—
Ti	—	1.05	2.7	0.7	—	—
W	1.8	—	—	—	—	—
V	0.24	1.3	—	—	—	—
C	0.13	0.06	—	0.03	0.1	—
B	—	0.2	0.01	0.01	—	—
Si	0.6	0.6	—	0.5	—	—
Cu	0.3	0.07	0.07	0.3	—	—
Mn	0.6	0.5	0.4	0.2	0.9	—
S	0.025	0.01	0.07	0.015	0.18	—
P	0.03	0.015	0.016	0.015	0.18	—
Ce	—	0.2	0.01	—	—	—
Pb	—	—	0.01	—	—	—
Nb + Ta	—	—	—	2.0	—	—
Zr	—	—	—	0.10	—	—
Sn + Sb	—	—	1.0	—	—	—

* Fe + Co.

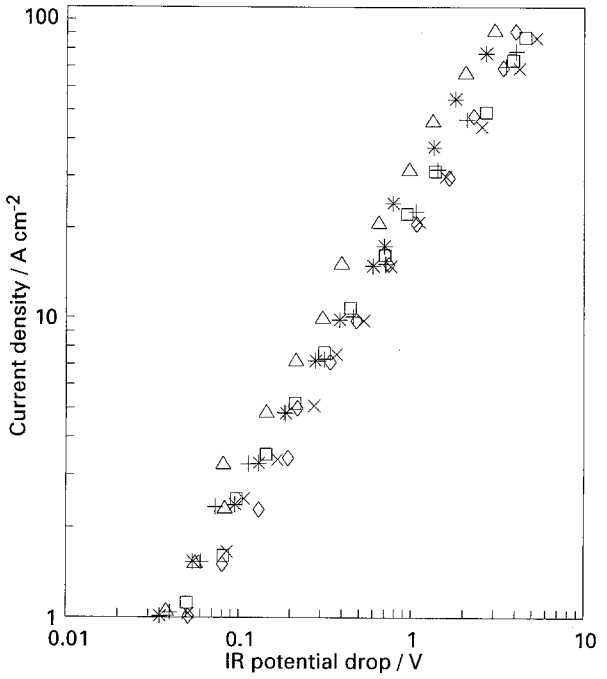

Fig. 6. Plot of *IR* potential drop against current density in 20% $NaClO_3$. The linear flow velocity of the electrolyte was 14 m s^{-1}, $Re = 7370$. (+) Mild steel, (*) AK1, (□) nickel, (×) LVN10, (◇) EI437 and (△) EI617.

electrode became bright and glossy. This observation is in good agreement with the finding of other authors [3, 24].

The polarization curves of the investigated materials in $NaClO_3$ solutions also exhibit Tafel behaviour. The break points on the polarization curves are visible in the case of EI617 and LVN10. The values of the double layer capacity do not exceed 40 μF cm^{-2} and the Tafel slope is in the range 24 to 88 mV. As can be seen from Figs 1 and 2, the *IR*-free anode potential of mild steel in $NaNO_3$ and $NaClO_3$ solutions neither reaches several volts as was previously reported [3, 4], nor does it have a negative slope [1]; both cases are at present, without any physically reasonable explanation.

The expected linear behaviour of the current density against ohmic potential drop in log–log coordinates can be seen from Figs 5 and 6. On the basis of the regression analysis using the equation

$$\log j = k_1 + k_2 \log(IR) \qquad (1)$$

where $k_1 = -0.38 \pm 0.08$ and $k_2 = 0.93 \pm 0.05$ for $NaNO_3$ and $k_1 = -0.56 \pm 0.06$ and $k_2 = 0.96 \pm 0.03$ for $NaClO_3$ (95% confidence interval), respectively.

Table 2. Average values of the Tafel slope and double layer capacity for the anode materials used, 20% $NaNO_3$

Anode material	*Tafel slope, b*/mV	*D.l. capacity, C*/μF cm^{-2}
Mild steel	13 ± 7	76 ± 9
AK1	22 ± 17	29 ± 4
Nickel	44 ± 19	11 ± 6
LVN10	35 ± 20	6 ± 3
EI437	46 ± 28	18 ± 6
EI617	93 ± 40	36 ± 8

Table 3. Average values of the Tafel slope and double layer capacity for the anode materials used, 20% $NaClO_3$

Anode material	*Tafel slope, b*/mV	*D.l. capacity, C*/μF cm^{-2}
Mild steel	88 ± 19	14 ± 5
AK1	39 ± 11	18 ± 6
Nickel	44 ± 17	8 ± 3
LVN10	50 ± 24	13 ± 3
EI437	24 ± 14	14 ± 7
EI617	68 ± 27	36 ± 8

This means that the estimated R value is independent of the applied current density.

4. Conclusion

The interruption technique was used for the estimation of the anodic potential of mild steel, nickel and four metal alloys at current densities up to 100 A cm^{-2} in a flow channel cell at Reynolds number 7370. Tafel kinetics [30] were suggested for the evaluation of transient values of the anodic potential. From the values of anodic potential vs current density Tafel slopes for all the materials were estimated. The Tafel slopes, $dE/d\log j$, are in the range 16 to 93 mV for 20% $NaNO_3$ solution and 24 to 88 mV for 20% $NaClO_3$ solution. On some of the *IR*-free polarization curves a plateau was observed, and the corresponding current density was denoted as the critical current density due to the formation of a salt film on the anode surface; this was supported by visual observation. The measured polarization curves can be used to calculate the local current densities during electrochemical machining of the studied materials [33].

References

[1] K. Chikamori, H. Yamamoto and S. Ito, Proceedings of the International Conference on *Production Engineering*, The Japan Society of Precision Engineering, Tokyo (1974), p. 68.
[2] A. D. Davydov, V. D. Kashcheav and R. A. Mirzoev, *Fizika i Khimiya obr. Mater.*, No. 3 (1974) 38.
[3] D. T. Chin and K. W. Mao, *J. Appl. Electrochem.* **4** (1974) 155.
[4] K. W. Mao and D. T. Chin, *J. Electrochem. Soc.* **121** (1974) 191.
[5] D. Landolt, *J. Electrochem. Soc.* **119** (1972) 708.
[6] A. D. Davydov, B. N. Kabanov, V. D. Kashchaev, R. A. Mirzoev and V. A. Nenaschev, *Fizika i Khimiya obrabotki mat*, No. 4 (1972) 139.
[7] A. D. Davydov and V. D. Kashchaev, *ibid.* No. 5 (1968) 40.
[8] D. T. Chin, *J. Electrochem. Soc.* **118** (1971) 174.
[9] D. Landolt, R. H. Müller and C. W. Tobias, *ibid.* **118** (1971) 40.
[10] D. Landolt, *ibid.* **119** (1972) 708.
[11] A. D. Davydov, K. D. Kascheaev, R. A. Mirozev, *Fizika i khimiya obrabotki mat.* No. 10 (1973) 32.
[12] K. W. Mao, *J. Electrochem. Soc.* **120** (1973) 1056.
[13] A. V. Vvedenskii, *Elecktronnaya obrabotka materialov*, No. 55 (1974) 79.
[14] M. L. McMillan and M. A. LaBoda, *J. Electrochem. Techn.* **5** (1967) 346.
[15] J. P. Hoare, M. A. LaBoda, M. L. McMillan and A. J. Wallace, *J. Electrochem. Soc.* **116** (1969) 199.

[16] J. P. Hoare, *ibid.* **117** (1970) 142.
[17] K. Chikamori and S. Ito, *Denki Kagaku* **38** (1970) 492.
[18] K. W. Mao, *J. Electrochem. Soc.* **118** (1971) 1870.
[19] K. W. Mao, *ibid.* **118** (1971) 1876.
[20] W. König and Degenhardt, 'Fundamentals of Electrochemical Machining' (edited by C. L. Faust), Electrochem. Society (1971).
[21] M. A. LaBoda, A. J. Chartrand, J. P. Hoare, C. R. Wiese and K. W. Mao, *J. Electrochem. Soc.* **120** (1973) 643.
[22] M. Datta and D. Landolt, *Corrosion Sci.* **13** (1973) 187.
[23] J. P. Hoare and C. R. Wiese, *ibid.* **15** (1975) 435.
[24] M. Datta and D. Landolt, *J. Electrochem. Soc.* **122** (1975) 1466.
[25] *Idem, ibid.* **124** (1977) 483.
[26] *Idem, J. Appl. Electrochem.* **7** (1977) 247.
[27] D. Landolt, *in* 'Passivity of Metals' (edited by J. Kruger and R. Frankenthal), Electrochem. Society, Princeton, NJ (1978) pp. 484–504.
[28] M. Datta and D. Landolt, *Electrochim. Acta.* **25** (1980) 1263.
[29] W. G. Clark and J. A. McGeough, *J. Appl. Electrochem.* **7** (1977) 277.
[30] J. Híveš and I. Rošar, *ibid.* **23** (1993) 1263.
[31] A. N. Frumkin, *Acta Physicochimica USSR* **18** (1943) 23.
[32] P. Novák, I. Roušar and R. Štefec, *Mater. Chem. Phys.* **10** (1984) 155.
[33] J. Híveš and I. Roušar, to be published.